*Canadian Mineralogist*
Vol. 18, pp. 251-259 (1980)

# ELECTRON CHANNELING AND ITS POTENTIAL FOR PETROFABRIC STUDIES

S. SAIMOTO
*Department of Metallurgical Engineering, Queen's University, Kingston, Ontario K7L 3N6*

H. HELMSTAEDT AND D. KEMPSON
*Department of Geological Sciences, Queen's University, Kingston, Ontario K7L 3N6*

E.M. SCHULSON*
*Materials Science Branch, Atomic Energy of Canada Limited, Chalk River Nuclear Laboratories, Chalk River, Ontario K0J 1J0*

## ABSTRACT

The electron-channeling method can be used for mineral-orientation analyses, and offers a new and potentially powerful petrofabric tool. Sample preparation requires the use of a low-speed cutting device to minimize damage to the surface atomic layers in which the channeling patterns are generated. The best results are obtained on minerals with relatively high electrical conductivity (*i.e.*, sulfides). Although electrical charge build-up presents a problem in silicates and carbonates, quartz and olivine yield good patterns after carbon coating according to standard practice. Once sample-preparation problems are overcome, the method may be applicable to other rock-forming minerals.

*Keywords*: petrofabric analysis, sulfides, scanning electron microscopy, electron channeling.

## SOMMAIRE

On peut se servir de la canalisation des électrons pour étudier l'orientation des cristaux; c'est un outil qui promet beaucoup dans les études de la pétrofabrique. La préparation d'un échantillon requiert un sciage à faible vitesse, afin de ne pas endommager les couches atomiques près de la surface, où se développe le phénomène de la canalisation. On obtient les meilleurs résultats sur espèces minérales à conductivité électrique élevée (sulfures, par exemple). Quoique la surcharge électrique soit un problème dans les silicates et les carbonates, le quartz et l'olivine donnent des clichés convenables si l'échantillon est enduit de carbone selon la technique ordinaire. Une fois les problèmes de la préparation d'un échantillon surmontés, la méthode pourrait s'appliquer à d'autres minéraux d'intérêt pétrologique.

(Traduit par la Rédaction)

*Mots-clés*: analyse de la pétrofabrique, sulfures, microscopie électronique à balayage, canalisation des électrons.

## INTRODUCTION

The study of preferred orientations of crystallographic directions in rock-forming minerals and sulfides is an important aspect of petrofabric analyses. For years the principal instrument for measuring the orientation of optically transparent minerals has been the petrographic microscope equipped with a universal stage (Emmons 1943). More recently, however, optical petrofabric methods have been increasingly supplemented by X-ray methods, in particular the use of the pole-figure goniometer (Starkey 1964, Baker *et al.* 1969, Phillips & Bradshaw 1970). X-ray methods not only have the advantage of measuring smaller grain sizes but, especially in the uniaxial minerals quartz and calcite, can provide (in addition to the optic-axis orientation) the position of other crystallographic directions necessary to give a full description of the fabric. Also, the pole-figure goniometer is an indispensable tool for the study of fabrics of optically opaque ore minerals (for a review, see Siemes 1977). Although the pole-figure goniometer measures the intensity of a selected plane within polycrystalline aggregates, it cannot perform the equivalent of axial distribution analyses, in which one explores the distribution of various direction groups within certain domains (Turner & Weiss 1963) and relate the orientation pattern to the texture of the sample. Expensive and time-consuming single-crystal methods would have to be employed to carry out such analyses by X-ray diffraction.

The present study investigates various procedures to obtain good-contrast electron-chan-

*Present address: Thayer School of Engineering, Dartmouth College, Hanover, New Hampshire 03755, U.S.A.

neling patterns with the scanning electron-microscope from rocks and minerals in order to facilitate petrofabric analyses. Discovered by Coates (1967), such patterns have been used successfully by metallurgists and material scientists for rapid-orientation determinations and microstructural studies (Schulson 1977). Although applications to geological materials have been few (Holt *et al.* 1968), the routine generation of such patterns from natural minerals would offer a new and potentially powerful petrofabric tool. The method would not only produce complete orientation analyses of small areas while holding the sample directly in view, but would also bridge the wide gap in scale between optical and transmission-electron microscopy.

The electron-channeling technique was reviewed recently by Schulson (1977), who presented a short summary of the channeling phenomenon and gave a detailed description of experimental procedures and the sample preparations necessary to obtain good channeling patterns from mineral and rock specimens. Examples of channeling patterns of several sulfide minerals as well as quartz and olivine were shown.

## Instrumental Principles

Consider first the principles of scanning electron current leaving the specimen is collected Figure 1. Electrons from a cathode (C) pass through a series of lenses (L) and focus on the surface of a specimen (S). A fraction of the electron current leaving the specimen is collected by a detector (P) and then passed to an amplifier (A), the output of which modulates the

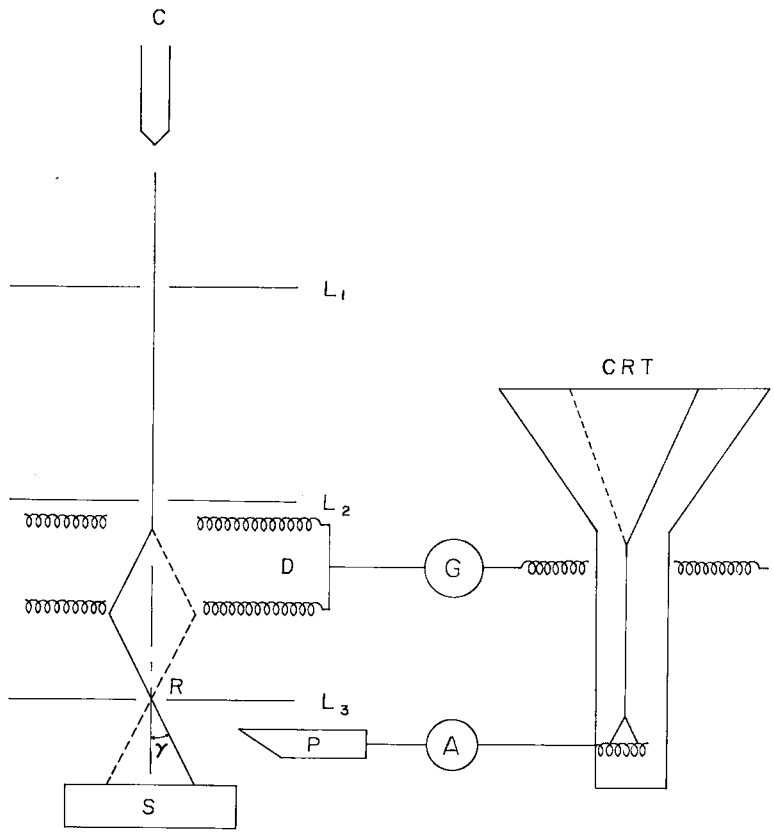


Fig. 1. Sketch of a scanning electron microscope: C is the cathode, L the lens, D the deflection coils, S the specimen, P the detector, G the scan generator, A the amplifier. The centre line of the incident electron-beam (both in the SEM column and in the CRT) is shown in two different positions to denote the different deflections at two different times.

brightness of a spot on a Cathode-Ray Tube (CRT) display. In passing along the column, the incident beam is deflected in two mutually perpendicular directions in synchronism with the spot on the display, so that a one-to-one correspondence exists between the probe position in S and the spot position. In this way, an image is produced.

For conventional topographic work, the probe is usually focused to a relatively small diameter ($l$), $\sim$ 10–20 nm, to give good spatial resolution, and it has a low divergence ($\delta$), $\sim 10^{-2}$ rad, resulting in a large depth of focus. The beam current ($i$) is then automatically set at $10^{-11}$–$10^{-12}$ A because the parameters are related through the brightness ($\beta$), which is a constant at all points along the optic axis; *i.e.*, $\beta = 0.4\, i/l^2\delta^2 \sim 2 \times 10^4$ Å/cm² sr (for a tungsten hairpin filament operating at 20 kV). For electron-channeling work, the probe is defocused and the divergence is even smaller ($\leqslant 10^{-3}$ rad). Correspondingly, the beam current is larger ($\leqslant 10^{-9}$ A). These changes reduce the spatial resolution but increase the signal-to-noise (S/N) ratio (S/N $\propto i^{1/2}$) and thus allow the electron-channeling effects, which are inherently low in contrast ($\leqslant 10\%$), to be detected in reasonably short (1–10 sec.) scan times. Moreover, the smaller divergence causes a greater fraction of the incident electron-beam to satisfy the channeling conditions for a given set of Bragg reflecting planes, a point that is made clearer below.

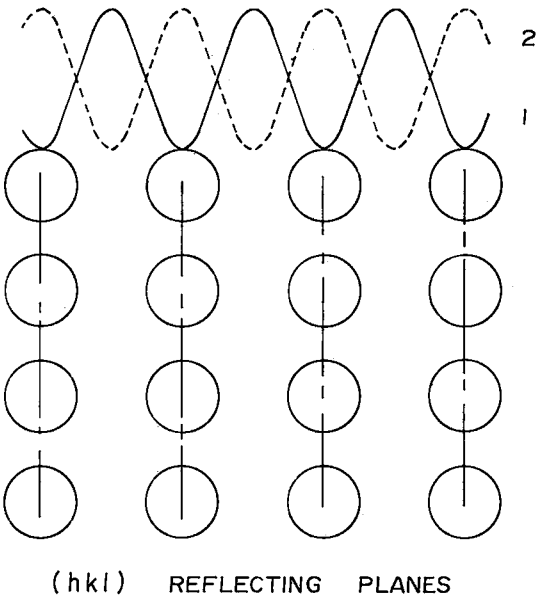


FIG. 2. Sketch of a crystal lattice through which Bloch waves 1 and 2 are propagating. The intensities of the two waves are equal, as shown, at the exact Bragg position, *i.e.*, $\theta = \theta_B$. Wave 1 is preferentially excited for $\theta > \theta_B$ and wave 2, for $\theta < \theta_B$.

## ELECTRON-CHANNELING PRINCIPLES

Consider next how electron channeling occurs. As discussed by Hirsch *et al.* (1965), the motion of an electron beam through a lattice can be described in terms of the propagation of Bloch waves, *i.e.*, plane waves that are modulated by the periodic potential of the crystal lattice. In the two-beam approximations, two waves are sufficient; wave 1 has nodes over the atomic positions and wave 2 has antinodes over these positions (Fig. 2). Both waves scatter and contribute to the back-scattered electron signal, but wave 1 has the lower scattering coefficient because its maxima in intensity avoid the atomic scattering centres. Thus, wave 1 may be viewed as the channeling wave and wave 2 as the absorbing wave.

Imagine now that the specimen is a large, single crystal having one set of Bragg reflecting planes perpendicular to the surface (Fig 3). When the direction of the incident beam exactly satisfies the Bragg conditions (*i.e.*, $\theta = \theta_B$, where $\theta_B$ is the Bragg angle for $\{hkl\}$ planes), both waves are excited equally. When $\theta > \theta_B$, however, wave 1 is preferentially excited, and when $\theta < \theta_B$ wave 2 is preferentially excited. Thus, when the beam passes through the Bragg positions during a single scanning sequence (which corresponds to a line scan in the conventional mode of operation), the depth of penetration into the lattice varies. So, too, does the back-scattered electron intensity, from a minimum when $\theta > \theta_B$ to a maximum when $\theta < \theta_B$. As this sequence continues throughout the complete frame scan, an electron-channeling line is built up on the CRT image, dark on one side and bright on the other. In reality, of course, there is more than one set of Bragg planes perpendicular, or nearly perpendicular, to the crystal surface, and so there is more than one channeling line generated. (It is assumed that the surface normal is parallel to the SEM optic axis. If not, then one must consider channeling about planes that are roughly parallel to the optic axis, not perpendicular to the crystal surface.) Indeed, as noted in Figure 3, scattering might even occur off the "front" and then, at a later time, off the "back" of the same $\{hkl\}$ set,

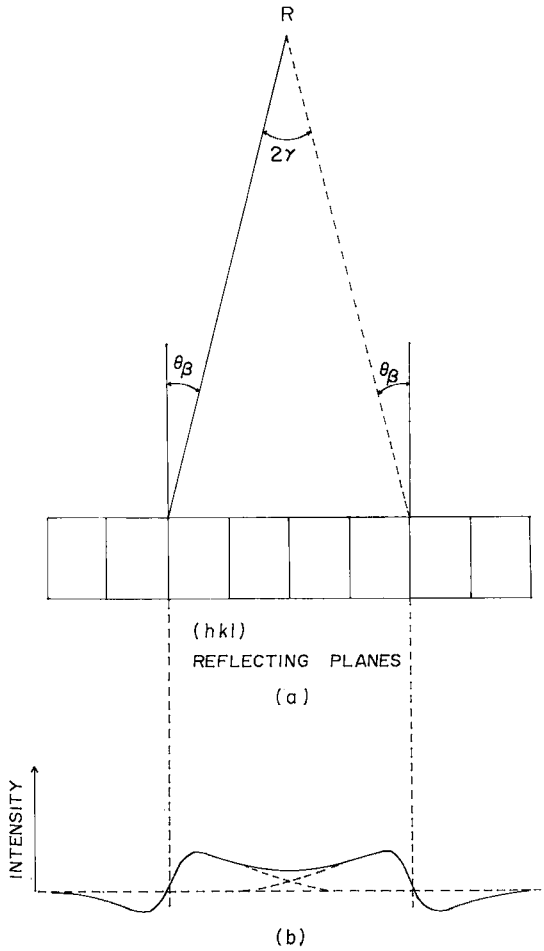


FIG. 3. Sketch showing (a) the electron beam incident on the specimen at the exact positions for diffraction from the "front" of the (*hkl*) reflecting planes at one time and from the "back" of the planes at a later time; and (b) the back-scattered electron intensity as a function of the direction of the incident electron-beam.

resulting in a pair of parallel lines separated by a {*hkl*} band of contrast, the centre and edge of which are brighter and darker than the background, respectively. This collection of lines and bands of contrast is termed an electron-channeling pattern (ECP).

Clearly, the greater the scanning angle, $2\gamma$ (Figs. 1, 3), the greater will be the chance of detecting a pole of symmetry. For indexing ease, therefore, $2\gamma$ should be as large as possible. In practice, the largest value of this parameter is usually approximately 10 to 15 degrees, and is determined by the highest current flowing through the deflection coils. In turn, this current is controlled by the lowest magnification setting on the SEM. From the foregoing discussion, it follows that one should view a channeling pattern as an angular map and not as a spatial map of the crystal. Each point on the pattern corresponds to a particular direction of incidence and not necessarily to a particular point on the specimen surface.

It also follows that pattern geometry provides a complete description of the crystallographic orientation of the area from which the pattern was generated. The methods used to analyze the patterns for determining the orientation have been described in the literature and will not be reiterated here. Computer programs (Young & Lytton 1972, 1977) can generate and plot ECP of any crystal lattice and thus facilitate the determination of orientation by comparing calculated and observed patterns.

## SELECTED-AREA CHANNELING PATTERNS (SACP)

If, instead of rocking the beam about a point (R) above the specimen surface (Figs. 1, 3), it is rocked about a point on the surface, the same scanning angle can be achieved about a fixed point. In this case, the ECP contrast is due solely to directional effects and not to a combination of spatial and directional effects. More importantly, this method of pattern generation allows crystallographic information to be obtained from areas that, in principle, may be as small as the beam size, *i.e.*, 1–2 $\mu$m in diameter. [As $l$, $\delta$ and $i$ are related, the requirements of high $i$ ($\geqslant 10^{-9}$ A) and of low $\delta$ ($\leqslant 10^{-1}$ rad) are the same for the selected-area, rocking-beam case as they are for the large-area, scanning-beam case.] In practice, however, the smallest areas from which patterns have been generated are 1–5 $\mu$m in diameter and, more commonly, between 10 and 50 $\mu$m, owing to "spherical"-aberration-type distortions that increase the effective size of the rocking point (Booker & Stickler 1972).

The rocking-beam method of pattern generation is affected (1) by cutting out the lower set of scanning coils (Fig. 1), (2) by increasing the diameter of the aperture in the final lens to $\sim$ 1–3 mm and (3) by using the final lens both to focus the beam and to deflect it back to a "point" on the SEM optic axis. The specimen is then positioned so that its surface and area of interest coincide with this point. To obtain a sufficiently well-collimated beam ($\delta \leqslant 10^{-3}$ rad), we reduced the diameter of the aperture in $L_2$ (Fig. 1) to $\sim$ 50–100 $\mu$m.

## Experimental Procedure

An AMR 900 scanning microscope was used for the present study, after suitable modifications to enable the bypassing of the compensating resistance in the condenser lens and the switching off of the lower scan coils for selected-area work. After much experimentation, it was found that a 20 kV accelerating voltage with condenser lens settings $L_1 \approx L_2 \approx 130$ mA for a specimen-to-objective lens pole-pieces distance of 1 mm (the minimum working-distance) produced good patterns on a (111)-oriented silicon wafer used as a reference specimen. The specimen-current mode was used because, at the very short working distances, the scintillator cannot readily receive the secondary electrons being emitted from the surface. In most cases, the aperture in the condenser lens (lens 2) was set at 100 $\mu$m. This procedure permitted patterns to be generated from selected areas of about 40 to 100 $\mu$m in diameter for a scanning angle of $\sim 20°$ with the magnification control set at x 20. Although the use of the 50 $\mu$m aperture in $L_2$ increased contrast slightly, it was considerably more sensitive to the condenser-lens setting and hence more difficult to image when examining polycrystalline specimens. This effect is due to alignment of the beam and can be minimized by re-alignment. However, for an instrument used most often as a standard SEM, it is more convenient to align the microscope for high resolution in standard scan and use the larger aperture for SACP study. When the working distance was increased to 3–4 mm, the $L_1$ and $L_2$ settings were 120 and 160 mA, respectively. Since the selected area for ECP decreases with a shorter working distance (Booker & Stickler 1972), flat specimens were placed in tall mounting stubs to ensure that they were almost touching the final pole-piece.

### *Surface preparation*

Electron channeling, as described above, is a phenomenon related to the few hundred atomic layers at the surface. If the specimen surface has been mechanically damaged, the patterns are either obliterated or severely blurred. Careful surface-preparation is therefore an important step in the procedure.

Although the use of standard geological polished sections would be most convenient, either no patterns or highly distorted images could be generated from such sections. Experimentation with different minerals revealed that this was primarily due to the damage caused by the initial, high-speed coarse saw-cut obtained when using a coarse diamond blade. Examination of fractured or cleaved surfaces showed that such surfaces allow patterns to be generated in the

TABLE 1

MINERALS WITH VARIOUS SURFACE PREPARATION EXAMINED BY SELECTED-AREA ELECTRON CHANNELLING

| CONDUCTING MINERALS | SURFACE PREPARATION | QUALITY OF SACP |
|---|---|---|
| CHALCOPYRITE | GEOLOGICAL POLISHED SECTION | VERY POOR TO NON-OBSERVABLE |
| PYRITE | GEOLOGICAL POLISHED SECTION | VERY POOR TO NON-OBSERVABLE |
| PYRITE (LARGE SINGLE CRYSTAL) | SPARK-MACHINED, METALLOGRAPHIC POLISH | GOOD |
| PYRITE (LARGE SINGLE CRYSTAL) | SPARK-MACHINED, METALLOGRAPHIC POLISH, ION BOMBARDMENT | VERY GOOD |
| PYRITE (FINE GRAINED) | SLOW DIAMOND CUT, METALLOGRAPHIC POLISH | FAIR |
| CHALCOPYRITE | FRACTURE | GOOD |
| GALENA | FRACTURE | GOOD |
| PYRITE (COARSE-GRAINED) | FRACTURE | GOOD |
| SPHALERITE | FRACTURE | GOOD |
| NON-CONDUCTING MINERALS AFTER CARBON COATING | | |
| CALCITE | FRACTURE | GOOD BUT DECAYS WITH CHARGE BUILD-UP |
| MICA (MUSCOVITE) | FRACTURE | GOOD |
| OLIVINE | SLOW DIAMOND CUT, METALLOGRAPHIC POLISH | POOR |
| OLIVINE | SLOW DIAMOND CUT, METALLOGRAPHIC POLISH, ION BOMBARDMENT | FAIR |
| QUARTZITE (COARSE GRAIN) | SLOW DIAMOND CUT, METALLOGRAPHIC POLISH | GOOD |
| QUARTZ (ARKANSAS SINGLE CRYSTAL) | STANDARD CUT, METALLOGRAPHIC POLISH | CHARGING |

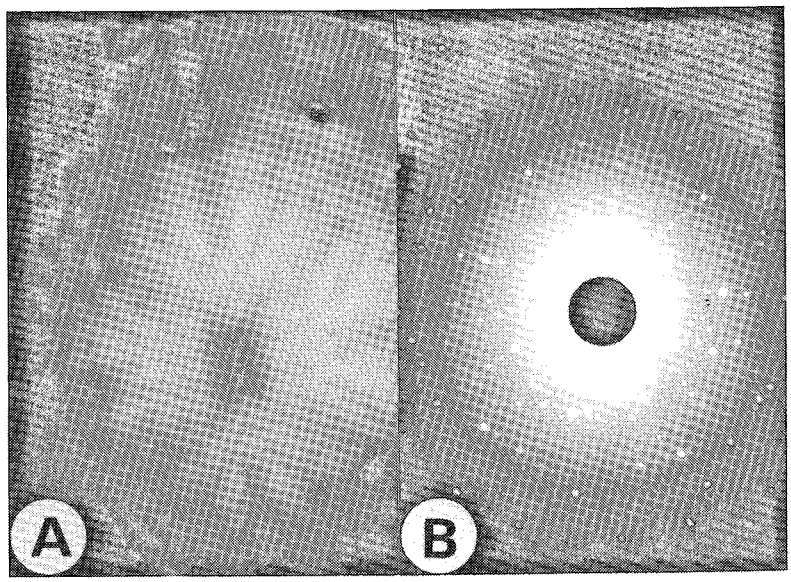


FIG. 4. (a) Selected-area channelling pattern from a large single crystal of pyrite after spark machining and polishing. (b) Laue back-reflection photograph of the same polished surface.

manner previously noted for alkali halide crystals (Schulson 1971). However, surface irregularities are a source of topographical disturbance, as their focal distance may differ from that of the working spot.

Experimentation with various surface finishes obtained by fracturing, polishing and chemical etching suggests that the ideal surface should be as smooth as possible. Mechanical damage during cutting was minimized by spark-machining (a cutting process limited to minerals whose resistivity is less than 100 ohm cm) or slow-speed cutting (0–300 rpm range) with a 270 grit diamond-impregnated saw. After cutting, approximately 0.2 mm was removed from the surface by standard metallographic polish (220, 320, 400, 600 silicon carbide papers followed by 3–0 and 4–0 emery paper, 6 $\mu$m diamond paste with a final 0.05 $\mu$m alumina polish). If, after polishing, images are still poor, further enhancement can be achieved by removing a few microns of the polished surface by ion bombardment. For this purpose, a standard apparatus available for the ion thinning of brittle materials was used.

## EXPERIMENTAL RESULTS

Table 1 summarizes the results on the minerals examined, and Figures 4, 5a and 6 show typical SACPs obtained. The surface-preparation technique described above made it possible to achieve routinely good to very good patterns from the relatively highly conductive sulfide minerals. The electron channeling should therefore be useful for axial-distribution analyses of sulfides. Figure 4 compares a channeling pattern of pyrite with a back-reflection Laue photograph of the same sample with the X-ray beam approximately along a diad axis. It can be seen that for orientation studies the SACP is a perfectly adequate substitute for the single-crystal X-ray photograph. Moreover, in addition to the orientation determination, all the other petrographic properties can be examined in the same grains, a clear advantage of the channeling technique.

Figure 5a shows a standard-scan image of a cleaved face of galena with a 200 $\mu$m diameter circle completely encompassing the region from which the SCAP (Fig. 5b) was taken. The diffuse diagonal line across the pattern is a defocused image of the cleavage step recognizable within the circle (Fig. 5a). The apertures used were $L_1 = L_2 = 100$ $\mu$m, $L_3 = 3$ mm with a working distance of about 1 mm. The condenser currents were 127 and 148 mA for $L_1$ and $L_2$, respectively. In this case the angular calibration of the SACP was accomplished by taking the SACP of a (111) silicon wafer

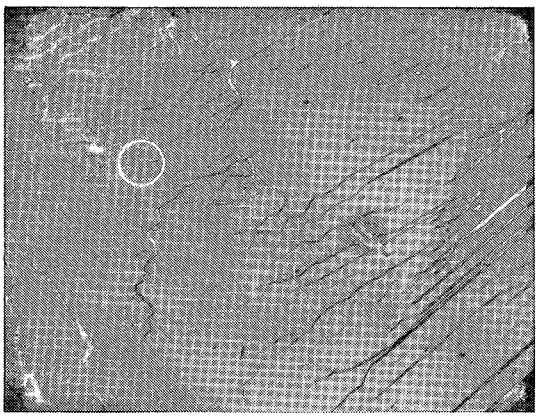

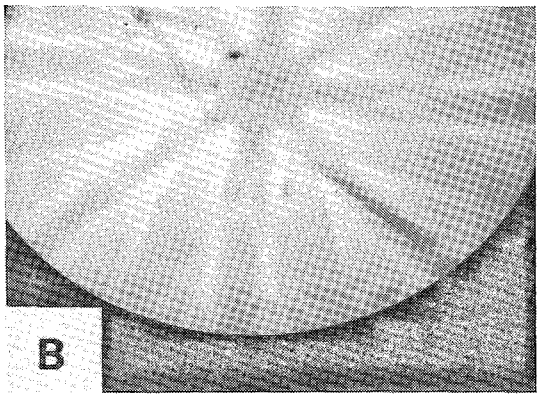

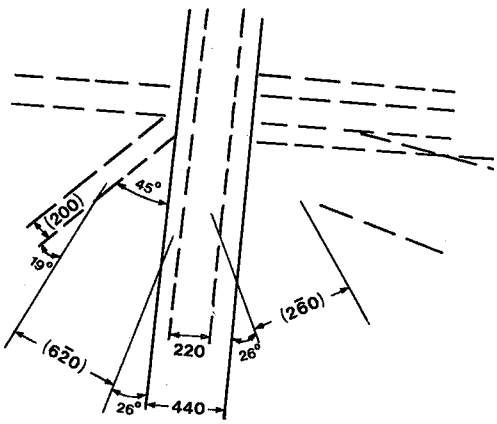


C

FIG. 5. (a) Standard-scan image of galena cleavage face. Circle (diameter 200 μm) is approximately 2 diameters larger than the spot size from which the SACP (Fig. 5b) was taken. (b) SACP of galena cleavage face (Fig. 5a). Apertures for $L_1 = L_2 = 100$ μm, $L_3 = 3$ mm. Condenser currents 127 and 148 mA for $L_1$ and $L_2$, respectively. Working distance 1 mm. (c) Trace of SACP (Fig. 5b) with indexed bands. Solid lines: distinct band edges; dashed lines: indistinct band edges.

mounted adjacent to the galena at the same working distance. Without any change in lens settings, a series of SACPs was taken by tilting the specimen stage up to 3°. This linear shift in the pattern $\triangle S$ *per* unit tilt $\triangle\beta$ in radians (258 mm/rad) is required to measure the total scanning angle $2\gamma = D\triangle\beta/\triangle S$, where $D$ is the length of the display-tube raster. The width of the band, as illustrated in Figure 3, is a measure of the Bragg angle: $2\theta_B = W(\triangle\beta/\triangle S)$. Hence, from the Bragg relation, $\lambda = 2d \sin\theta_B$ and, for small angles, $d_{(hkl)} = \lambda\triangle S/W\triangle\beta$. The wavelength $\lambda$ is determined from the de Broglie relation, and has been tabulated for various energizing voltages (Hirsch *et al.* 1965). The 20 kV used in the present case corresponds to a $\lambda$ of 0.0859 Å. A trace of the SACP is shown on Figure 5c. The band edge of the second order (440) is the sharpest, and ratios of the measured spacings agree with those calculated using 5.935 Å for the lattice constant of this $B1$-type structure. Also, the angular measurement of 26° between {6$\bar{2}$0} and {440} is close to the expected value of 26.6°. The bands with a markedly tapered appearance contained within {6$\bar{2}$0} correspond to {4$\bar{2}$0}. Because of the curved nature of the bands, their widths should be measured near the centre of the image. The four-fold symmetry is obvious from the SACP, and the zone axis is [002]. With the silicon standard, it was found that the absolute values of the $d$ determined are within only 10% of the calculated value, suggesting that a comparison of spacing ratios eliminates the error in the $\triangle S/\triangle\beta$ determination. The most accurate method of measuring this parameter is to tilt without losing the imaged spot and to make a double exposure.

Although this study was initiated to measure the orientation of rock-forming minerals, experiments with the electrically resistive silicates and carbonates revealed problems of electrical charging caused by the slow drainage of the impinging electrons. Charging can be suppressed by carbon-vapor deposition, and the thickness of the coating can be gauged by the degradation of the patterns of a simultaneously coated silicon crystal as a standard. The degree of charge suppression depends on the conductivity of the specimen, but the thickness of the coating should not exceed $\sim$ 10 nm.

Even after carbon coating, charging may persist. For example, Arkansas quartz of high purity charged excessively, whereas a quartzite (Selwyn Range, Alberta) did not charge at all and yielded good SACPs (Fig. 6a). SACPs of olivine (Fig. 6b) are not as distinct as those

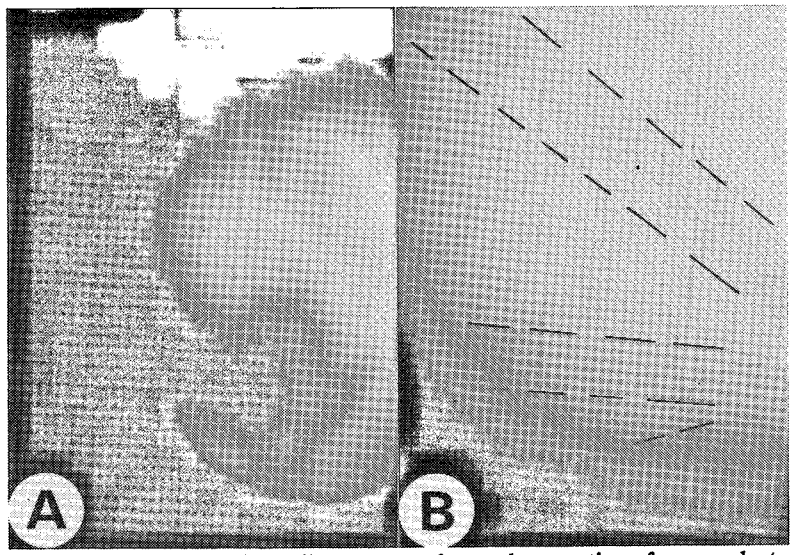


FIG. 6. Selected-area channeling pattern after carbon coating of nonconducting materials: (a) quartzite (Selwyn Range, Alberta) and (b) olivine (dunite, Norway).

of quartz, suggesting that olivine is less resistant to abrasion damage. Although SACPs of carbon-coated calcite were plainly visible, after a few minutes a charge build-up occurred, and interfered with normal photographic recording. This phenomenon is similar to that found earlier by Schulson (1971) on alkali halide crystals. A photographic record can be taken, however, if a special high-persistence phosphor CRT display is used in conjunction with a camera to photograph the display. In this procedure some contrast and angular resolution are lost, but the quality of the SACP should be sufficient to determine the crystallographic orientation.

## DISCUSSION

Initial results show that routine generation of electron-channeling patterns is possible in sulfides, as long as caution is observed during surface preparation. For the first time, it will be possible to perform sulfide petrofabric analyses analogous to universal-stage analyses of optically transparent minerals. Difficulties in locating grain boundaries during the channeling procedure can be solved by noting the $x$–$y$ coordinates whenever the patterns change, indicating that a boundary is being transversed.

Although charging problems persist, the fact that it has proved possible to obtain patterns from quartz, calcite and olivine is encouraging. Work is continuing in order to overcome the charging problem and to make the method applicable to petrofabric analyses of the major rock-forming minerals.

Information other than the crystal orientation may be obtained from SACP by quantitative measurement of the channeling line-widths (Joy & Booker 1973). The line becomes more diffuse and broadens as the distortion in the crystalline matrix increases. With large irregular distortion the patterns are obliterated, as occurred with standard geological polished sections. If the surface preparation minimizes the surficial damage, this technique could be used to measure the degree of inherent elastic distortion found in the mineral from one crystallite to another, or from one region to another in the same crystallite. This means that a map of the crystallites showing spatial orientation and degree of elastic distortion in each may be constructed. This procedure would be analogous to determining the $c$-axis distribution in quartzite and noting which crystallites manifest undulatory extinction. In the SACP method, the orientation determination is without rotational ambiguity and could be developed to determine the axis of bend that gives rise to the undulatory extinction. The present study was undertaken to develop such a technique, which would facilitate the axial distribution study of subgrains in quartz. Initially, microfocus X-ray photos were

prepared for this purpose, but the exposure time necessary to obtain an analyzable photograph was over eight hours. SACP, once it is applicable routinely, will shorten considerably the time needed for such microstructural analyses.

## Acknowledgements

We are thankful for financial support for this work through a Queen's University Advisory Research Committee grant, a National Research Council Co-op grant and National Research Council Grant *A*8375. We thank Mr. Peter Fryzuk of the Department of Energy, Mines and Resources for preparing the ion-bombarded specimens.

## References

Baker, B.W., Wenk, H.-R. & Christie, J.M. (1969): X-ray analysis of preferred orientation in fine-grained quartz aggregates. *J. Geol.* **77**, 144-172.

Booker, G.R. & Stickler, R. (1972): Scanning electron microscope selected-area channelling patterns; dependence of area on rocking angle and working distance. *J. Mat. Sci.* **7**, 712-714.

Coates, D.G. (1967): Kikuchi-like reflection patterns obtained with the scanning electron microscope. *Phil. Mag.* **16**, 1179-1184.

Emmons, R.C. (1943): The universal stage. *Geol. Soc. Amer. Mem.* **8**.

Hirsch, P.B., Howie, A., Nicholson, R.B., Pashley, D.W. & Whelan, M.J. (1965): *Electron Microscopy of Thin Crystals.* Butterworths, London.

Holt, D.G., Gavrilović, J. & Jones, M.P. (1968): Scanning-electron-beam anomalous transmission patterns. *J. Mat. Sci.* **3**, 553-558.

Joy, D.C. & Booker, G.R. (1973): Recent developments in electron channelling techniques. *Proc. Sixth Ann. Scanning Electron Microscopy Symp.* I, 137-143.

Phillips, F.L. & Bradshaw, R. (1970): The use of X-rays in petrofabric studies. *In* Experimental and Natural Work Deformation (P. Paulitsch, ed.), Springer-Verlag, Berlin.

Schulson, E.M. (1971): A scanning electron microscope study of the degradation of electron channelling effects in alkali halide crystals during electron irradiation. *J. Mat. Sci.* **6**, 377-383.

——— (1977): Electron channelling patterns in scanning electron microscopy. *J. Mat. Sci.* **12**, 1071-1087.

Siemes, H. (1977): Fabric analysis and fabric development in ores. *Geol. Fören. Stockh. Förh.* **99**, 172-185.

Starkey, J. (1964): An X-ray method for determining the orientation of selected crystal planes in polycrystalline aggregates. *Amer. J. Sci.* **262**, 735-752.

Turner, F.J. & Weiss, L.C. (1963): *Structural Analysis of Metamorphic Tectonites.* McGraw-Hill, New York.

Young, C.T. & Lytton, J.L. (1972): Computer generation and identification of Kikuchi projections. *J. Appl. Phys.* **43**, 1408-1417.

——— & ——— (1977): Computer generation and identification of divergent beam diffraction phenomena. *Int. Conf. Computer Simulation for Materials Application; Nuclear Metallurgy* **20**(2), 1244-1253.

*Received March 1979, revised manuscript accepted February 1980.*